

Article

Green Synthesis of Copper Oxide Nanoparticles Using *Sesbania grandiflora* Leaf Extract and Their Evaluation of Anti-Diabetic, Cytotoxic, Anti-Microbial, and Anti-Inflammatory Properties in an In-Vitro Approach

Kanagavalli Ramasubbu ¹, Siddharth Padmanabhan ¹, Khalid A. Al-Ghanim ², Marcello Nicoletti ³, Marimuthu Govindarajan ^{4,5,*} , Nadezhda Sachivkina ⁶  and Vijayarangan Devi Rajeswari ^{1,*} 

¹ Department of Biomedical Sciences, School of Biosciences and Technology, Vellore Institute of Technology, Vellore 632014, TN, India; kanaga0497@gmail.com (K.R.); siddharthpadmanabhan50@gmail.com (S.P.)

² Department of Zoology, College of Science, King Saud University, Riyadh 11451, Saudi Arabia; kghanim@ksu.edu.sa

³ Department of Environmental Biology, Sapienza University of Rome, 00185 Rome, Italy; marcello.nicoletti@uniroma1.it

⁴ Unit of Mycology and Parasitology, Department of Zoology, Annamalai University, Annamalainagar 608002, TN, India

⁵ Unit of Natural Products and Nanotechnology, Department of Zoology, Government College for Women (Autonomous), Kumbakonam 612001, TN, India

⁶ Department of Microbiology V.S. Kiktenko, Peoples Friendship University of Russia (RUDN University), Moscow 117198, Russia; sachivkina@yandex.ru

* Correspondence: drgovind1979@gmail.com (M.G.); vdevirajeswari@vit.ac.in (V.D.R.)



Citation: Ramasubbu, K.; Padmanabhan, S.; Al-Ghanim, K.A.; Nicoletti, M.; Govindarajan, M.; Sachivkina, N.; Rajeswari, V.D. Green Synthesis of Copper Oxide Nanoparticles Using *Sesbania grandiflora* Leaf Extract and Their Evaluation of Anti-Diabetic, Cytotoxic, Anti-Microbial, and Anti-Inflammatory Properties in an In-Vitro Approach. *Fermentation* **2023**, *9*, 332. <https://doi.org/10.3390/fermentation9040332>

Academic Editor: Ronnie G. Willaert

Received: 5 March 2023

Revised: 20 March 2023

Accepted: 23 March 2023

Published: 27 March 2023



Copyright: © 2023 by the authors. Licensee MDPI, Basel, Switzerland. This article is an open access article distributed under the terms and conditions of the Creative Commons Attribution (CC BY) license (<https://creativecommons.org/licenses/by/4.0/>).

Abstract: Green methods of synthesizing nanoparticles are safer than chemical and physical methods, as well as being eco-friendly and cost-efficient. In this study, we use copper oxide nanoparticles (CuO NPs) fabricated with *Sesbania grandiflora* (Sg) (Hummingbird tree) leaves to test the effectiveness of green synthesizing methods. The attained Sg-CuO NPs physical and optical nature is characterized by UV-Vis spectroscopy Differential Reflectance Spectroscopy (UV-Vis DRS), Fourier Transform Infra-Red spectroscopy (FTIR), X-ray Diffraction spectroscopy (XRD), Scanning Electron Microscope (SEM), and Energy Dispersive X-ray Analysis (EDAX). UV-Vis spectrum for Sg-CuO NPs revealed a peak at 410 nm. SEM images showed the aggregation of needle-shaped particles, at a size of 33 nm. The amylase and glucosidase enzymes were inhibited by the Sg-CuO NPs up to 76.7% and 72.1%, respectively, indicating a possible antihyperglycemic effect. Fabricated Sg-CuO NPs disclosed the excellent inhibition of DPPH-free radicle formation (89.7%) and repressed protein degradation (81.3%). The results showed that Sg-CuO NPs display good anti-bacterial activity against the gram-negative (*Escherichia coli* and *Pseudomonas aeruginosa*) and gram-positive (*Staphylococcus aureus*). Cytotoxicity of the Sg-CuO NPs was determined using an IC₅₀ of 37 µg/mL. Sg-CuO NPs have shown promising anti-diabetic, anti-oxidant, protein degradation-inhibiting, and anti-microbial properties. Our findings have shown that synthesized Sg-CuO NPs have biological activities that may be utilized to treat bacterial infections linked to hyperglycemia.

Keywords: nanotechnology; green synthesis; medicinal plant; antihyperglycemic; bioactivity; anticancer

1. Introduction

Nanotechnology focuses on synthesizing nanomaterial, and has diverse application, such as biomedicine, delivery of nutrients and drugs, imaging techniques, etc. Multiple methods are available for nanoparticle synthesizing, including chemical processes, sol-gel, laser ablation, electro biosynthesis, biological, and green synthesis. In the green synthesis method of nanoparticles, instead of chemicals, plant-mediated products are likely to play the role of reducing agents; green reducing agents lessen the toxic effects of chemicals in the

environment and are cost-effective [1,2]. Furthermore, selecting a suitable reducing agent is necessary to promote the nanoparticles' medicinal properties and reduce the accumulation of heavy metals [3]. Cu nanoparticles (Cu NPs) nanoparticles are widely used and efficient in reducing the reactive oxygen species' (ROS) mediated oxidative stress [4].

Sesbania grandiflora (English: Hummingbird tree, Tamil: Agathi) has been reported to have various biological activities. It is widely known for its anti-diabetic, anti-ulcerative, anti-microbial, and anti-oxidant properties [5]. Primary (carbohydrates, proteins, and lipids) and secondary metabolites (alkaloids, phenols, tannins, and coumarins) were found to enhance their biological activity [6]. *S. grandiflora* inhibits the carbohydrate metabolic enzyme from regulating hyperglycemia [7], as well as reducing oxidative stress and free radical formation, and acting on the inflammatory cytokines [8,9]. Moreover, *S. grandiflora* and its mediated nanoparticles like ZnO, Ag, and TiO inhibit the growth of pathogenic microorganisms: *Staphylococcus aureus*, *Salmonella enterica*, *Burkholderia* sp. *Escherichia coli*, and *Bacillus* sp. [10,11]. Bacterial and fungal infections are generally treated using antibiotics and anti-fungal agents. However, excessive usage of antibiotics mutates the microbes to develop resistance and destroys the microbiota, which leads to multiple sub-problems. Therefore, it is necessary to develop some alternative treatment methods.

Chronic hyperglycemia and the metabolic condition of diabetes mellitus (DM) are closely related. Chronic hyperglycemia alters the cellular and metabolic functions of the body. It negatively impacts several organs and causes microvascular and macrovascular complications [12], such as immune compromise, retinopathy, nephropathy, neuropathy, renal diseases, and cardiovascular diseases. In uncontrolled diabetic conditions, immune system dysfunctions affect innate immunity and humoral immunity, which increases oxidative stress and reduces the response of T-lymphocytes, neutrophils, and inflammatory cytokines [13,14]. IL-1, IL7, IL 12, IL 33, TNF α , and IFN γ deplete in hyperglycemic conditions; this allows bacterial infection and increases the intracellular bacterial load [12]. Due to this immune-compromised state, diabetic patients tend to frequently experience further medical conditions; foot ulcers and infections in the urinary tract, skin, throat, and stomach caused by bacteria and fungi are the most common. They are susceptible to hospital-born or opportunistic infections, such as *S. aureus*, *E. coli*, *Streptococcus aeruginosa*, *Klebsiella pneumonia*, and *Mycobacterium tuberculosis* [15–17]. Furthermore, diabetic patients are likely more vulnerable to COVID-19 infection and sepsis [18,19].

Trace elements are revealed to improve immunity, reduce oxidative stress and inflammation, and improve insulin resistance. Cu, Zn, Fe, Co, Mg, Mn, Cr, and Se all act as cofactors in various metabolic and signal transduction pathways [20]. Metal oxide NPs are an excellent alternative to antibiotics due to their stability and nontoxic nature [20]. Cu is critical in hyperglycemia, insulin secretion, mechanism and action, oxidative stress, and immunity. The Zn and Cu act on oxidative stress by regulating the superoxide dismutase (SOD), oxidases, and peroxidases; these enzymes reduce free radical production, maintain homeostasis, and reduce oxidative stress [20,21]. Cu is reported to restore the pancreatic β cell islets, as well as promote insulin secretion and the inflammatory response by elevating the secretion of interleukins. Its deficiency influences the respiratory chain; simultaneously affects ATP production, glucose intolerance, hypertension, and lipid metabolism; and increases ROS and reactive nitrogen species, mitochondrial dysfunction, and apoptosis [21,22]. Because of their biological activities, physical properties, and chemical nature, metal oxide NPs, particularly Cu, have a critical role in biomedicine [23].

This study focuses on Cu as a significant source for treating hyperglycemia and its related complications. Based on the available literature about *S. grandiflora* and its biological activity (specifically on antihyperglycemic and anti-microbial activities), and cost efficiency, we chose this plant to fabricate Sg-CuO NPs. We then confirmed and characterized the nanoparticles using relevant techniques, such as UV-Vis Differential Reflectance Spectroscopy DRS, Fourier Transform Infra-Red spectroscopy (FTIR), X-ray Diffraction (XRD), Scanning Electron Microscope (SEM), and Energy Dispersive X-ray Analysis (EDAX).

These techniques further analyzed fabricated CuO nanoparticles' antihyperglycemic, antimicrobial, anti-oxidant, anti-inflammatory, and cytotoxic properties.

2. Materials and Methods

2.1. Chemicals

Fresh leaves of *S. grandiflora* were brought from the local market in Vellore, Tamil Nadu, India. Copper sulfate (99.8% pure), alpha-glucosidase (1 U/mL), sodium carbonate (extra pure), and nutrient agar were purchased from SRL chemicals, India. Alpha-amylase, starch soluble, and dinitro salicylic acid (DNSA) (98% pure), as well as 2,2'-diphenyl-1-picrylhydrazyl (DPPH) (extra pure, 95%), were sourced from Himedia, India. We bought ascorbic acid, diclofenac, and metformin from Sigma Aldrich. Phosphate buffer (pH, 6.6) was prepared with sodium phosphate dibasic (0.5 M) and sodium phosphate monobasic (0.5 M). Gram-negative (*E. coli* and *P. aeruginosa*) and gram-positive (*S. aureus*) bacterial cultures were collected from the Vellore Institute of Technology–Vellore, Tamil Nadu, India. Distilled water was used for the preparation of the solution in the experiments. All the assays were performed in triplicates.

2.2. Preparation of Leaf Extract and CuO Nanoparticles

The *S. grandiflora* plant was authenticated and certified (authentication no PARC/2-22/4735) by Dr. P. Jayaraman, who worked at the Plant Anatomy and Research Center, Chennai, TN, India. To obtain *S. grandiflora* water extract, we boiled approximately 26 g of the powdered leaf in 200 mL of distilled water for 1 h. CuO nanoparticles were synthesized using this extract. In addition, 6 g of *S. grandiflora* leaf powder was extracted with water, methanol, hexane, and chloroform for phytochemical analysis.

We then added 45.5 mL of 0.1M copper sulfate with 100 mL *S. grandiflora* prepared water extract while stirring at 60 °C. To eliminate the contaminants, we prepared *S. grandiflora* green synthesized CuO nanoparticle (Sg-CuO NPs), which was then centrifuged at 5000 rpm for 10 min. For 48 h, the recovered pellet was calcined at 100 °C [24]. This sample was sonicated for 30 min in distilled water for further assays.

2.3. Phytochemical Analysis

Extracts of *S. grandiflora* were tested for their phytochemical content (primary and secondary metabolites) using the following techniques [25–28].

2.3.1. Test for Primary Metabolites

Fehling's test: Equal volume of extracts were mixed with Fehling's (A and B) reagent, and heated for 3 to 5 min. Red precipitate indicated the existence of carbohydrates.

Iodine test: 2 mL of *S. grandiflora* extract was mixed with the 2 mL of iodine solution and potassium iodide (Lugol solution). The development of the blue color showed the presence of starch [27].

Biuret test: The 1 mL extract was mixed with a few drops of 3% copper sulfate and 10% sodium hydroxide. The red or violet color formation indicated the presence of proteins or peptides [27].

2.3.2. Test for Secondary Metabolites

Salkowski's test: H₂SO₄ was added to the test tube's walls after shaking 1 mL of *S. grandiflora* extracts with chloroform. The appearance of red color indicated the presence of steroids [25].

Mayer's test: The appearance of a yellow or white color, after adding 2–3 drops of Mayer's reagent to 1 mL of various solvent extracts of *S. grandiflora*, suggested the presence of alkaloids [27].

Wagner's test: In 5 mL of distilled water, we dissolved 2 g of potassium iodide and 1.2 g of iodine. This solution was then diluted with 100 mL of distilled water. The 1 mL of each

extract was mixed with a few drops of this mixture. The development of brown-colored precipitates indicated the presence of alkaloids [26].

Ferric chloride test: 2 mL of extracts and a few drops of 5% ferric chloride solution were mixed. The formation of a blue solution revealed the presence of phenols [25].

NaOH test: 3 mL of 10% NaOH was mixed with 1 mL of *S. grandiflora* extracts. The formation of yellow color indicated the presence of coumarins [28].

Lead acetate test (10%): Lead acetate 10% was combined with plant extracts in a 1 mL volume. The presence of flavonoids was shown by yellow precipitation.

Lead acetate test (1%): Two to three drops of 1% lead acetate and 0.5 mL of various *S. grandiflora* extracts were combined. The production of a white precipitate confirmed the presence of tannin [28].

2.4. Physical and Optical Characterization of Nanoparticles

Green synthesized Sg-CuO NPs was optically characterized with UV-Visible Diffuse Reflectance Spectroscopy (UV-Vis DRS) (Jasco V-630, Oklahoma, OK, USA), Fourier Transform Infra-Red (FTIR) (Thermo Nicolet iS50 with inbuilt ATR, Shimadzu, Kyoto, Japan) with the spectra range was in between 4000 cm^{-1} to 500 cm^{-1} , X-ray Diffraction spectroscopy (XRD) (Bruker D8 Advance, Bruker, Germany), Scanning Electron Microscope (SEM) (EVO/18 Research, Carl Zeiss, Jena, Germany), and Energy Dispersive X-ray Analysis (EDAX) (ZEISS EVO18).

2.5. Anti-Hyperglycemic Assay

2.5.1. Alpha-Amylase Inhibition Activity

Various concentrations of sonicated Sg-CuO NPs (20–100 $\mu\text{g}/\text{mL}$) and metformin (20–100 $\mu\text{g}/\text{mL}$), the standard drug (as positive control), were incubated with the *v/v* of 2 mM phosphate buffer (pH 6.6). A measurement of 1 mL of α -amylase was incubated for 20 min; we then added 500 μL of the 1% starch solution to the reaction mixture, followed by the 5 min of incubation. 1 mL of DNSA was then mixed and incubated for 5 min in the boiling water bath. α -amylase inhibition was measured in UV-Vis spectrophotometer at 540 nm [29]. The equation below was used to calculate the inhibitory activity of Sg-CuO NPs.

$$\% \text{ of inhibition} = (\text{Control} - \text{Test}) / \text{Control} \times 100 \quad (1)$$

2.5.2. Alpha-Glucosidase Inhibition Assay

The 96-well plate contained five doses of 10 μL sonicated Sg-CuO NPs (20–100 $\mu\text{g}/\text{mL}$), 30 μL of 2 mM phosphate buffer, and 10 μL of α -glucosidase. The incubation followed at 25 °C for 10 min. As a substrate, 50 μL of 3 mM P-nitrophenyl glucoside was added and left for 20 min at 37 °C. Further, by mixing 50 μL of 0.1 M, the Na_2CO_3 reaction was stopped, and we then determined the color intensity with a microplate reader at 405 nm. A well without a sample but with buffer, substrate, and enzyme was employed as a negative control. [30], while metformin was used as a positive control. With Equation (1), the inhibitory activity of α -glucosidase was determined.

2.6. Anti-Oxidant Assay-DPPH

A 96-well microtiter plate was used to test the Sg-CuO NPs ability to scavenge free radicals with the DPPH method. A measurement of 0.1 M DPPH was then prepared with methanol. A measurement of 200 μL of 0.1M DPPH was added to the microtiter plate and 15 μL of Sg-CuO NPs at five different concentrations (ranging from 20 to 100 $\mu\text{g}/\text{mL}$). Ascorbic acid (20–100 $\mu\text{g}/\text{mL}$) in a volume of 15 μL was employed as a positive control. The microtiter plate was incubated at 25 °C in the dark for 30 min. Afterward, we read the plate in a spectrophotometer plate reader at 517 nm [31]. We then calculated the free radical scavenging activity with Equation (1).

2.7. Anti-Inflammatory Assay

The anti-inflammatory activity of Sg-CuO NPs was investigated with the albumin degradation assay. Albumin was taken from the fresh hen egg white, while 0.2 mL of egg white, 2.8 mL of phosphate buffer (pH, 6.4), and different concentrations of 2 mL of Sg-CuO NPs (20–100 µg/mL) were mixed and incubated at 37 °C for 15 min, and at 70 °C for 5 min. Here distilled water was taken as a negative control, while metformin (20–100 µg/mL) and diclofenac (20–100 µg/mL) were taken as a positive control. This mixture was measured at 660 nm in a spectrophotometer [32]. Protein degradation inhibition was measured in percentage with the given equation.

$$\% \text{ of inhibition} = ((\text{Test})/(\text{Control}) - 1) \times 100 \quad (2)$$

2.8. Anti-Bacterial Activity

The anti-bacterial properties of Sg-CuO NPs (50–125 µg/mL) were analyzed with the disk diffusion method against the standard streptomycin (10 mg) on a nutrient agar medium. The bacterial strains, gram-negative (*E. coli* and *P. aeruginosa*) and gram-positive (*S. aureus*), were inoculated in the Petri dishes, followed by the 20 µL of Sg-CuO NPs. The plates were then incubated for 24 h at 37 °C [33]. After incubation, the zone of inhibition (diameter) was measured with image J.

2.9. Cytotoxicity Assay

Cytotoxicity of the Sg-CuO NPs was measured based on the reducing capability of 3-(4,5-dimethylthiazol-2-yl)-2,5-diphenyl tetrazolium bromide (MTT) to form formazan, a purple-blue precipitate formed in the HepG2 cell line. Various concentrations of Sg-CuO NPs (10–100 µL/mL) and cisplatin as a positive control were incubated with 20 µL of MTT (5 mg MTT in an ml of PBS) for 4 hrs. It may have resulted in forming formazan, which was dissolved with 200 µL of DMSO, and it was later measured in a spectrophotometer at 570 nm [34]. The viability of the cells was calculated with:

$$\% \text{ of cell viability} = (\text{Test}/\text{Control}) \times 100 \quad (3)$$

Further, to differentiate between the alive and dead cells, treated HepG2 cells were seeded into the six-well plate and incubated with AO/EtBr dual stain for 10 min at dark. The cells were then observed under fluorescence microscopy.

2.10. Statistical Analysis

All the statistical representations were performed using JMP pro, origin pro, and Graphpad prism software. The results were analyzed using two-way ANOVA and Tukey's post hoc *t*-test (≤ 0.05). Images were processed in Image j software (ImageJ, v1.54c bundled with 64-bit Java 8).

3. Results

3.1. Physical and Optical Characterization

Mixing copper sulfate and *S. grandiflora* leaf extract at constant temperature and stirring turned the red plant extract into dark green and black after calcination. Calcination aided in forming the structure and shape of the nanoparticles characterized by UV-Vis DRS, FTIR, XRD, SEM, and EDAX.

3.1.1. UV-Vis Spectroscopy Differential Reflectance Spectroscopy

UV-Vis DRS analyzed the absorption of light on the surface of the Sg-CuO NPs and the energy gap (Eg). Eg was measured using UV-vis DRS with the help of a tauc plot.

$$Ah\nu = E (h\nu - E_g)^{1/2} \quad (4)$$

The band energy gap was calculated as 1.006 eV (Figure 1). The UV range for this nanoparticle was 200–800 nm, and the maximum absorption occurred near 410 nm. It is similar to the UV range of CuO NPs. It discloses the presence of CuO NPs [35,36]. *S. grandiflora* leaf extract might act as a stabilizer, reducer, and capping agent, reducing the copper sulfate hexahydrate to copper oxide nanoparticles.

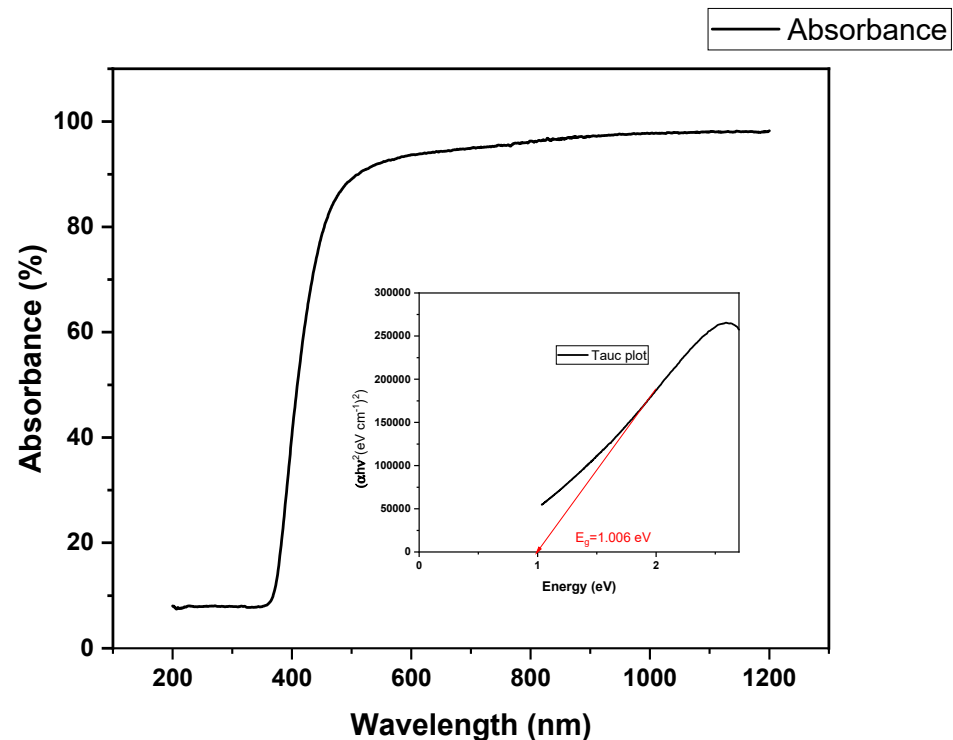


Figure 1. UV-Vis spectroscopy DRS of Sg-CuO NPs with Tauc plot for calculating the excitation energy.

3.1.2. Fourier Transform Infra-Red Spectroscopy (FTIR)

The FTIR spectrum of fabricated CuO nanoparticles showed broadband in 3226 and 2937. Sharp peaks at 1595 cm^{-1} , 1401 cm^{-1} , 1091 cm^{-1} , and 612 cm^{-1} in this spectrum represent C-O stretching, O-H bending, and C=C stretching, respectively (Figure 2); functional groups are present in the produced CuO NPs. This IR spectrum reveals that carboxylic acid, proteins, carbohydrates, nucleic acids, flavonoids, phenols, and alkaloids act as a capping agent for the nanoparticles, and reduce and stabilize them [24]. These metabolites and compounds maintain the nanoparticles' structure in alkaline conditions [37].

3.1.3. X-ray Diffraction

Peaks from XRD confirm that the formed nanoparticles were in the crystalline phase. A total of 2θ values (35.1θ , 38.3θ , 48.2θ , 61.1θ , and 74.7θ) analyzed from heights gave the assigned values of 111, 111, 200, 113, and 220 (Figure 3). These are similar to the results of Liu et al. It also reveals that the formed nanoparticles were not pure Cu, consisting of Cu and CuO NPs [38]. Furthermore, crystallinity of Sg-CuO NPs from XRD was calculated with the following equation:

$$\text{Crystallinity} = \text{Area of crystalline peaks} / \text{Area of all peaks (crystalline + amorphous)} \times 100 \quad (5)$$

Our results reveal that the synthesized nanoparticles have very low crystallinity (4.56%) and might be amorphous. Distinctive XRD pattern peaks also support this claim [39].

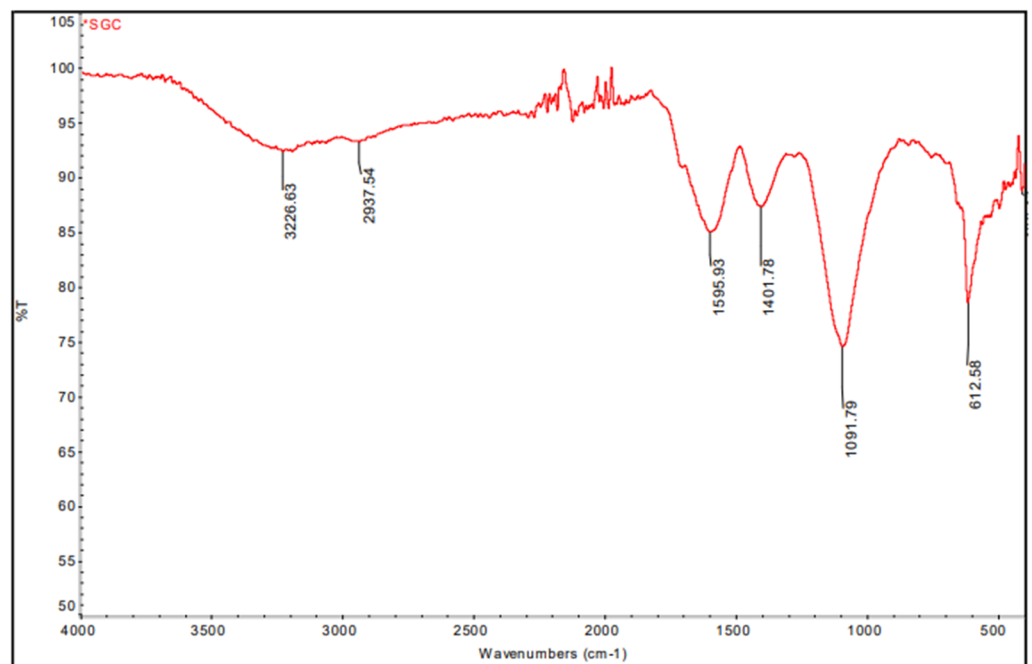


Figure 2. FTIR spectrum of Sg-CuO NPs.

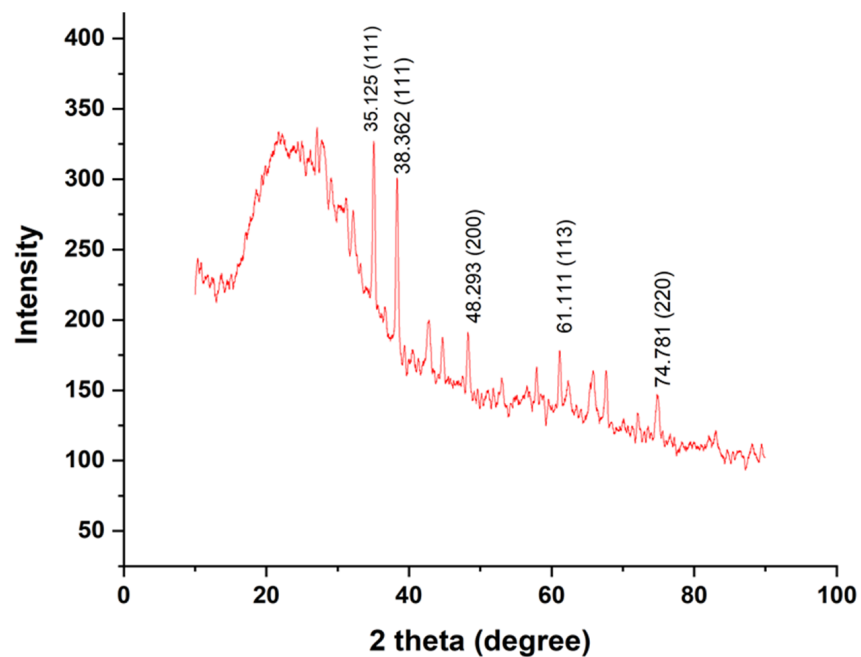


Figure 3. X-ray diffraction spectroscopy peaks of Sg-CuO NPs.

3.1.4. Scanning Electron Microscopy

SEM results showed that the formed nanoparticles were needle-shaped (Figure 4a,b). Based on these results, the average diameter and length of the formed Sg-CuO NPs were measured with image J software as 33 nm and 1051 nm (Figure 4c,d). CuO nanoparticles' size came within the range of previously produced dispersed nanoparticles. [40]. Moreover, the nanoparticles were agglomerated; this might be due to their small size, increased surface area, and various biomolecules [41].

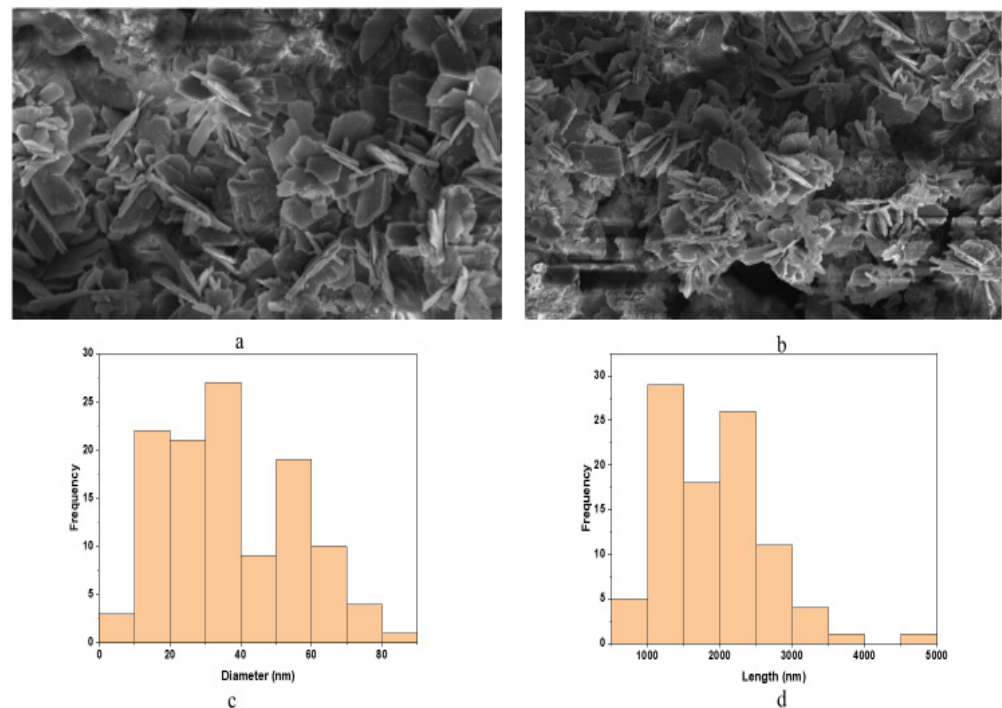


Figure 4. Scanning electron microscope (SEM) image of *Sg*-CuO NPs at 2 μm and 3 μm (a,b). (c,d) are the graphical representations of the diameter and length of the formed needle-shaped nanoparticles size measured with image J software, which gave the average diameter of the nanoparticle as 33 nm, and the average length as 1051 nm.

3.1.5. Energy Dispersive X-ray Analysis (EDAX)

Energy dispersive X-ray analysis (EDAX) is a technique connected with SEM. It is used for determining elemental composition. The fabricated nanoparticles observed under EDAX revealed the Cu and O present in the *Sg*-CuO NPs as 78% and 28% (Figure 5). This ratio is close to the 2:1 ratio of the previously reported studies [42].

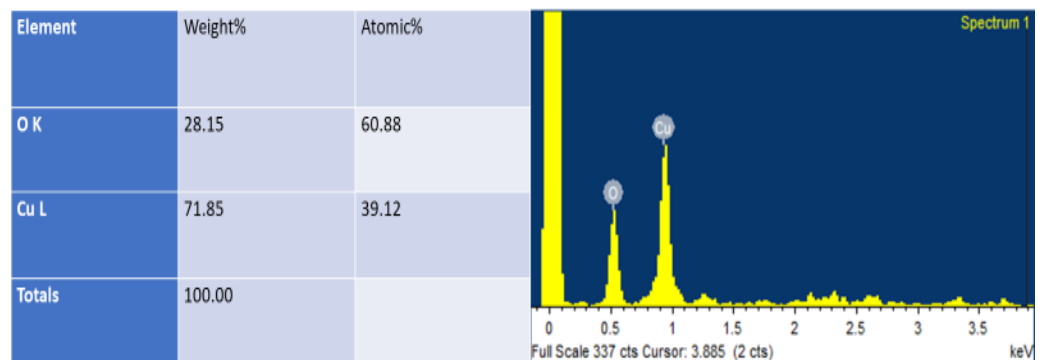


Figure 5. Energy dispersive X-ray Analysis (EDAX) results of *Sg*-CuO NPs.

3.2. Phytochemical Analysis

The phytochemical content of any plant depends on its environment, growth conditions, soil, water availability, etc. These factors have a critical role in the plant’s applications, particularly in medical applications. Phytochemical content analysis is essential to identifying the drug-like biomolecules within the plant [43]. Moreover, phytochemicals have a critical role in the formation of nanoparticles. Primary (carbohydrates, proteins, lipids, and nucleic acids) and secondary metabolites (flavonoids, alkaloids, phenols, terpenoids, etc.) were reported to bind with the metal NPs to stabilize their structure [44]. Here we have

prepared four different extracts (water, methanol, hexane, and chloroform) for analyzing the phytochemical content of *S. grandiflora*. Aqueous and methanolic extracts of *S. grandiflora* showed promising results compared to the hexane and chloroform extracts. Phytochemical assays with aqueous and methanolic extracts indicated the presence of alkaloids, carbohydrates, phenols, flavonoids, and tannins. Meanwhile, hexane and chloroform extracts do not contain flavonoids, tannins, coumarins, and carbohydrates (Table 1). Flavonoid compounds quercetin, kaempferol, sativan, and phenolic resveratrol were reported previously in the *S. grandiflora* methanolic extract [45], which largely reflects the results manifested here.

Table 1. Phytochemical content of the *Sesbania grandiflora* extracts.

Name of the Test	Phytochemicals	Water Extract	Hexane Extract	Methanol Extract	Chloroform Extract
Mayer's test	Alkaloids	+	+	+	-
Wagner's test	Alkaloids	+	+	+	-
Fehling's test	carbohydrate	+	-	+	-
Iodine test	carbohydrate	+	+	+	-
Biuret test	Peptides	-	-	-	-
Salkowski's test	Steroids	-	-	+	+
FeCl ₃ test	Phenols	+	+	+	-
NaOH test	Coumarins	+	-	-	-
10% lead acetate	Flavonoids	+	-	+	-
1% lead acetate	Tannins	+	-	+	-

3.3. Anti-Hyperglycemic Activity

α -amylase and α -glucosidase break down carbohydrates into disaccharides and oligosaccharides in the intestine. This process leads to the elevation of the glucose in the blood, and causes hyperglycemia in diabetic patients. Furthermore, hyperglycemia elevates the glucose released from the liver for metabolic activity. However, the lack of insulin action elevates the glucose level [1]. The most common diabetic drugs target these enzymes to reduce hyperglycemia. Trace elements (Cu and Zn) and vitamins (vitamins C and D) are reported to regulate insulin secretion and insulin sensitivity, and reduce glucose absorption in the digestive tract [22,46]. Furthermore, to confirm this, fabricated Sg-CuO NPs enzyme inhibitory activity to minimize glucose absorption was observed. It was revealed to inhibit the activity of α -amylase and α -glucosidase up to 76% and 72% at the highest concentration (100 μ g/mL), which is similar to the effects of the most common diabetes drug metformin at 100 μ g/mL. It ranges from 20% to 76.7% for α -amylase, and 32% to 72.1% for the α -glucosidase (Figure 6). This result is similar to *Cocculus hiesutus*-mediated CuO NPs [1]. Compared with the fungal-mediated CuO NPs, it showed better enzyme inhibitory activity [40]. Therefore, it is suitable to treat hyperglycemia by influencing the carbohydrate metabolic enzymes (α -amylase and α -glucosidase). The study reveals that the Sg-CuO NPs lowers glucose absorption, indirectly impacting blood glucose levels.

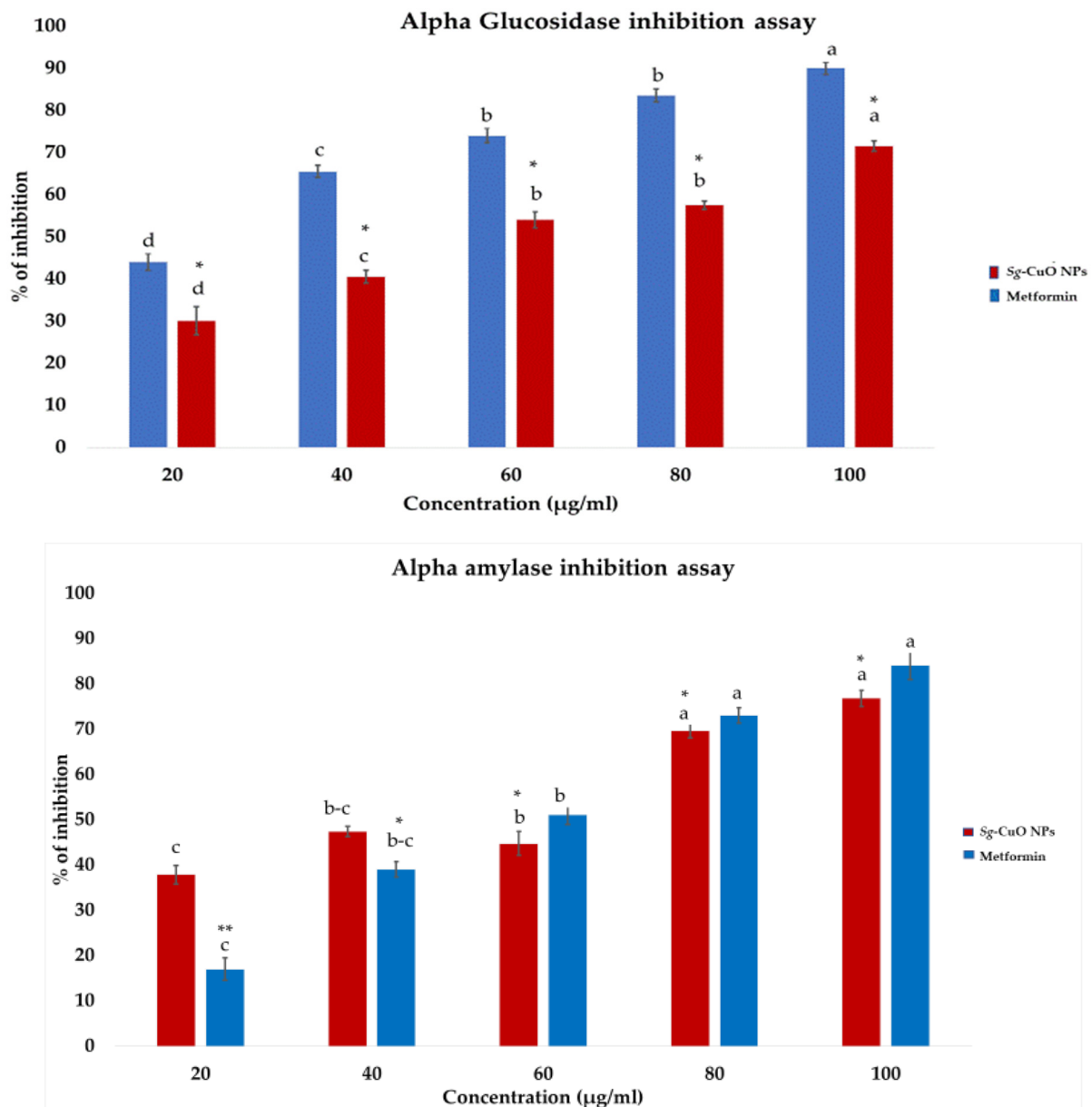


Figure 6. α -glucosidase and α -amylase inhibitory activity of Sg-CuO NPs (20–100 $\mu\text{g}/\text{mL}$) and the standard drug metformin (20–100 $\mu\text{g}/\text{mL}$). Values expressed in mean \pm SD, ANOVA followed by Tukey’s post hoc, which showed a significant level p -value * < 0.001 , ** < 0.05 (Lowercase letters).

3.4. Anti-Oxidant Activity

Oxidative stress caused by hyperglycemia promotes various complications, such as inflammation, elevated insulin resistance, and mitochondrial dysfunction. The metabolic processes generate superoxide anions, hydrogen peroxide, nitric oxide, and hydroxy radicals. The processes also impact lipid peroxidation, protein oxidation, DNA replication, and break strands [9]. Further oxidative stress leads to cellular dysfunctions and metabolic impairments, and modulates the immune system by interfering with the mechanism of action of macrophages, neutrophils, and lymphocytes [47]. It also advances microbial infections. Thus, reducing ROS generation and chelating it is necessary. Studies conducted in in vitro systems would only be applicable in some cases due to the difference between the biological and in vitro environments [48]. Nonetheless, discovering the compound’s anti-oxidant and free radical chelating activity in the in vitro methods is the most reliable, time-saving, and resource-preserving method. DPPH is a free radical used for the in vitro

analysis of most anti-oxidant studies because of its stable free radical nature. Free radical scavenging activity of the Sg-CuO NPs was observed as 30% to 89.7% with a concentration range of 20–100 $\mu\text{g}/\text{mL}$ (Figure 7). It is higher than the scavenging activity of *S. grandiflora* extracts, aqueous extract (80%), and ethanolic extract (83%) [49]. *Millettia pinnata* green synthesized CuO NPs showed 86% scavenging activity [4]. It specifies that Sg-CuO NPs and other green synthesized nanoparticles were better for reducing the free radical formation.

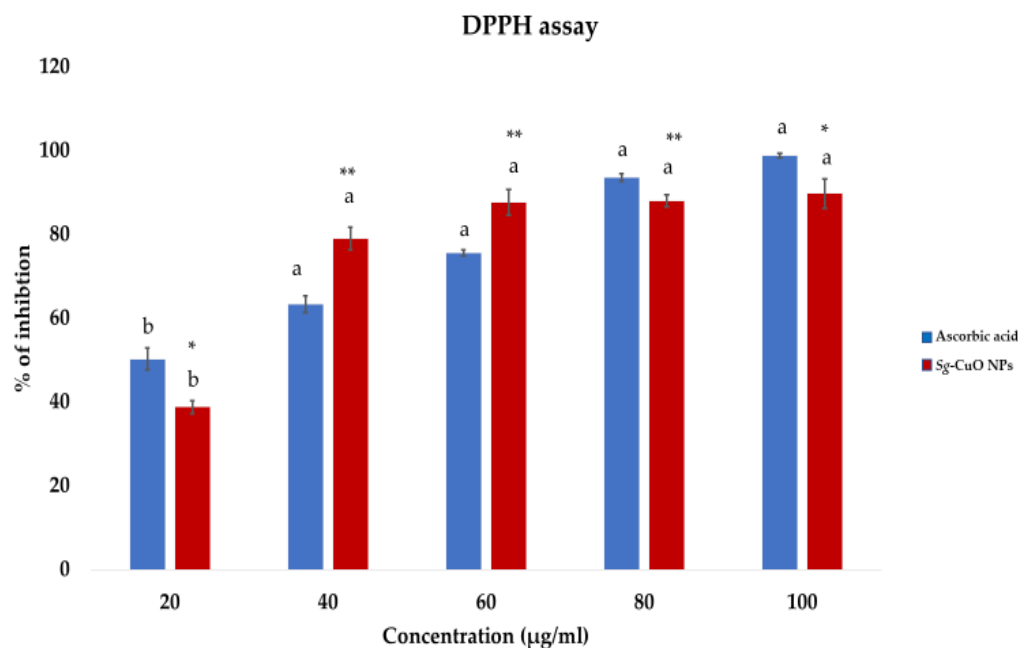


Figure 7. DPPH free radical scavenging activity of Sg-CuO NPs (20–100 $\mu\text{g}/\text{mL}$) plotted against the ascorbic acid (20–100 $\mu\text{g}/\text{mL}$) (positive control). Values expressed in mean \pm SD, ANOVA followed by Tukey's post hoc, which showed a significant level p -value * < 0.001, ** < 0.05 (Lowercase letters).

3.5. Protein Degradation Assay

DM increases inflammation and promotes tissue damage in several ways, such as protein misfolding, protein denaturation, lipid peroxidation, and hemolysis [4]. Hyperglycemia induces the production of advanced glycation end products, oxidative stress, insulin resistance, inflammatory cytokines, and frequent infections [50]. In hyperglycemic conditions, glycation and oxidation of proteins elevate inflammation, causing cell injury and damage [51]. Protein degradation occurs when the physicochemical changes modify the primary (e.g., peptide bond) and secondary bonds (e.g., hydrophobic, electrostatic, and disulfide bonds) [32]. Thus, reducing protein degradation by maintaining the bonds between the amino acids may help regulate inflammation. Cu is proven to be critical in this via insulin and glucose metabolism.

Furthermore, it reported elevating insulin sensitivity while regulating lipid metabolism and coronary heart diseases [52]. In this study, egg albumin was used as a protein source. Its denaturation was measured against diclofenac (non-steroidal anti-inflammatory drug) and metformin, a standard diabetic medicine reported to reduce inflammation. The protein denaturation assay revealed that Sg-CuO NPs exhibits anti-inflammatory activity by decreasing protein degradation. Protein denaturation inhibition of Sg-CuO NPs ranged from 34.8% to 81.3% for the 20–100 $\mu\text{g}/\text{mL}$ concentrations. This result is similar to the anti-inflammatory activities of the diabetic drugs metformin (85.9%) and diclofenac (94%). Increasing the Sg-CuO NPs protein denaturation concentration seems to lessen inflammation (Figure 8). Psomas et al. stated that anti-oxidants of trace elements like Cu and Zn are useful, and have no or fewer side effects [53]. Other investigations mentioned that Cu interaction with COX 2 and glutathione peroxidase in biological conditions might significantly reduce oxidative stress and protein degradation. Further studies need to

be performed in natural conditions (in vitro or in vivo) to find the actual mechanism of Sg-CuO NPs in reducing inflammation [54], as our results offer a promising starting point for reducing protein degradation and inflammation in hyperglycemic scenarios.

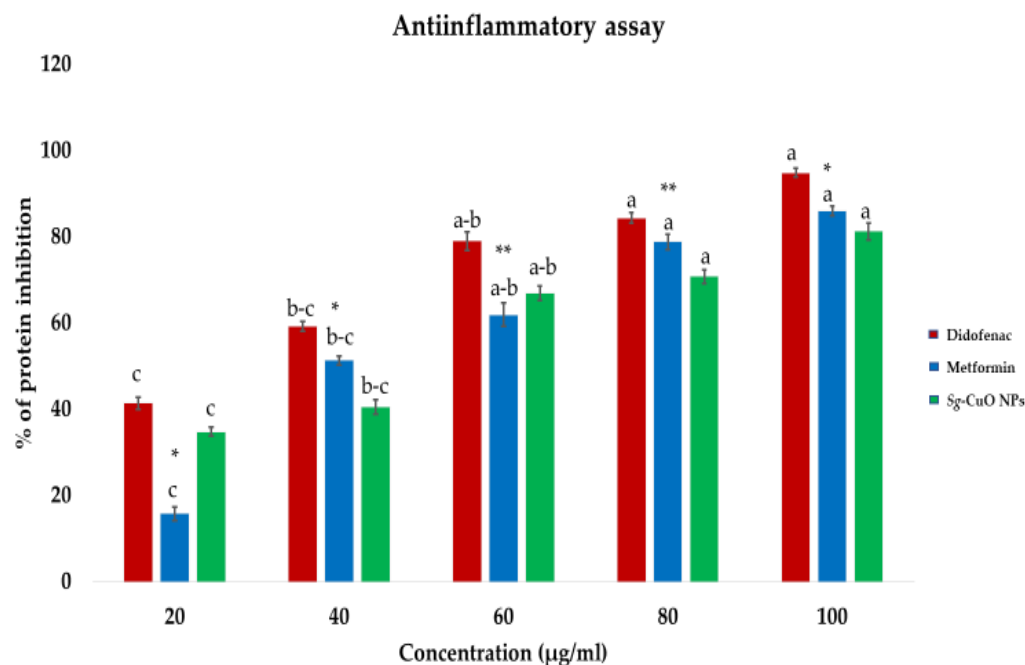


Figure 8. Egg albumin degradation test for protein degradation with Sg-CuO NPs (20–100 µg/mL) against the positive controls metformin (20–100 µg/mL) and diclofenac (20–100 µg/mL). Values expressed in mean ± SD, ANOVA followed by Tukey’s post hoc, which showed a significant level at p -value * < 0.001, ** < 0.05 (Lowercase letters).

3.6. Anti-Bacterial Property

Bacterial infections in diabetic patients are one of the significant causes of hyperglycemia. Bacterial infections delay wound healing and causes diabetic ulcers, urinary infections, and lung infections. Moreover, oxidative stress and inflammation in diabetes worsen bacterial infections. In the current scenario, antibiotic resistance pathogens languish the treatment for bacterial infection [55]. These circumstances advance the need for developing alternative treatment methods, such as metal nanoparticles, Cu, Zn, Au, and Ag, which are primarily known for their anti-microbial activity. Synthesized Sg-CuO NPs was investigated for its anti-bacterial activity. Metal ions like CuO NPs bind with the lipid membrane and induce oxidation. This further collapses the membrane to leak the intracellular contents [42,55,56]. Evidence suggests that CuO and Cu₂O cause damage to the cell wall and interfere with the functions of enzymes, such as the iron-sulfur enzyme family and fumarase A. Formation of these protein complexes might inhibit the growth of the bacteria [57]. The anti-bacterial activity of Sg-CuO NPs was analyzed with *E. coli*, *P. aeruginosa*, and *S. aureus* against streptomycin (10 mg). In this assay, the anti-bacterial activity of three different concentrations of Sg-CuO NPs (50, 100, and 125 µg/mL) was analyzed by disk diffusion method (Figure 9).

According to the results, increasing the concentration decreased the organism’s growth. This is due to the dose-dependent response of the Sg-CuO NPs against the chosen organisms. Sg-CuO NPs inhibited the growth of *E. coli* at 100 and 125 µg, and formed a zone of inhibition 10 ± 1.21 mm and 14 ± 1.39 mm in diameter for each concentration. It showed a predominant result compared to streptomycin (17 ± 0.46 mm). The zone of inhibition against *P. aeruginosa* has been measured as 17 ± 0.45 mm and 19 ± 0.94 mm at 100 and 125 µg/mL, respectively. Compared to streptomycin (20 ± 1.38 mm), Sg-CuO NPs showed excellent anti-bacterial activity. Meanwhile, against *S. aureus*, Sg-CuO NPs revealed a

remarkable anti-bacterial activity. The zone of inhibition was evaluated as 12 ± 1.1 mm, 14 ± 1.1 mm, and 15 ± 1.5 mm for 50, 100, and 125 $\mu\text{g}/\text{mL}$, respectively. Remarkably, 125 μg showed a promising result after 24 hrs for *E. coli* (14 ± 1.39 mm), *P. aeruginosa* (19 ± 0.94 mm), and *S. aureus* (15 ± 1.5 mm). Based on these results, The anti-bacterial activity of the Sg-CuO NPs is quite similar to that of Cu nanodots, and CuO nanoparticles acted on the multi-drug-resistant bacteria [55,58]. Like the *S. grandiflora*, CuO nanoparticles fabricated with it also inhibited gram-positive and gram-negative bacterial growth [59].

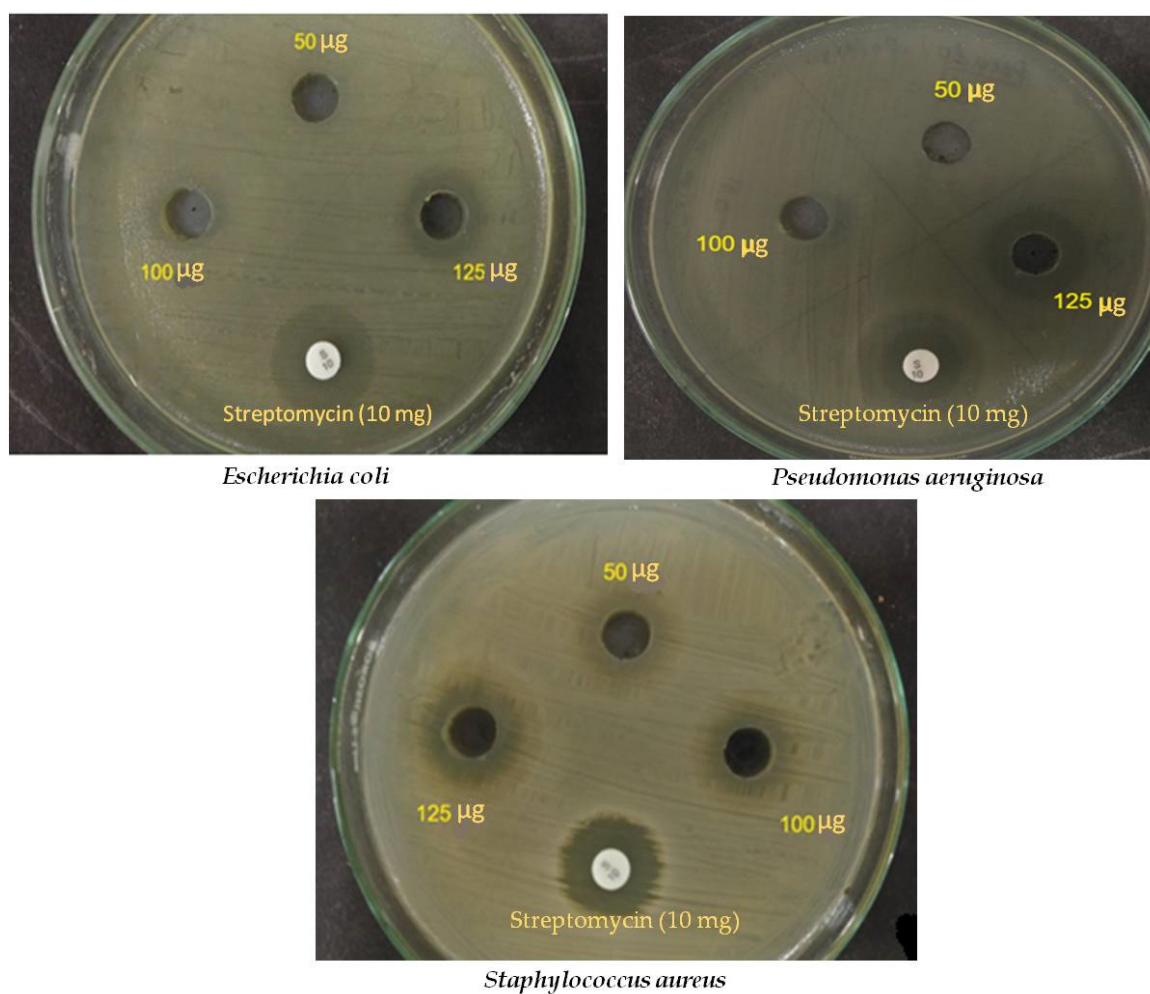


Figure 9. Anti-bacterial activity of Sg-CuO NPs (50, 100, and 125 $\mu\text{g}/\text{mL}$) against *E. coli*, *P. aeruginosa*, and *S. aureus*. Streptomycin 10 mg was used as a control.

3.7. Cytotoxicity

Toxicity studies have a crucial role in drug development; expected adverse effects of the drugs can be determined through toxicity analysis. Chronic exposure to drugs and chemicals is monitored to identify their toxic effects. In silico, in vitro, and in vivo analysis methods have been used to determine these adverse effects [60]. Toxicity depends on the period of exposure to the drug, molecular structure, size of the particle, chemical nature, accumulation, its interaction with the body, etc.; here, we have taken the different concentrations of Sg-CuO NPs (10–100 $\mu\text{g}/\text{mL}$) to identify whether this dose can induce apoptosis in the HepG2 hepatocellular carcinoma cells. MTT was reduced by the succinate dehydrogenase in the alive cells to an insoluble product called formazan, which can be measured with spectrophotometry [61]. When the concentration of the Sg-CuO NPs was increased, apoptosis of the cells was observed. IC_{50} of the Sg-CuO NPs was calculated as 37 μg in HepG2 cells (Figure 10). However, this might vary between different types of cell

lines. similar-sized (40–60 nm) nanoparticles showed discrete in between the HepG2, A549, and SH-SY5Y cell lines. Thus, before exploring its possibilities as a hyperglycemic and anti-bacterial candidate, an extensive study must be performed in various cell lines, and to discover its possible bioavailability at in vivo conditions.

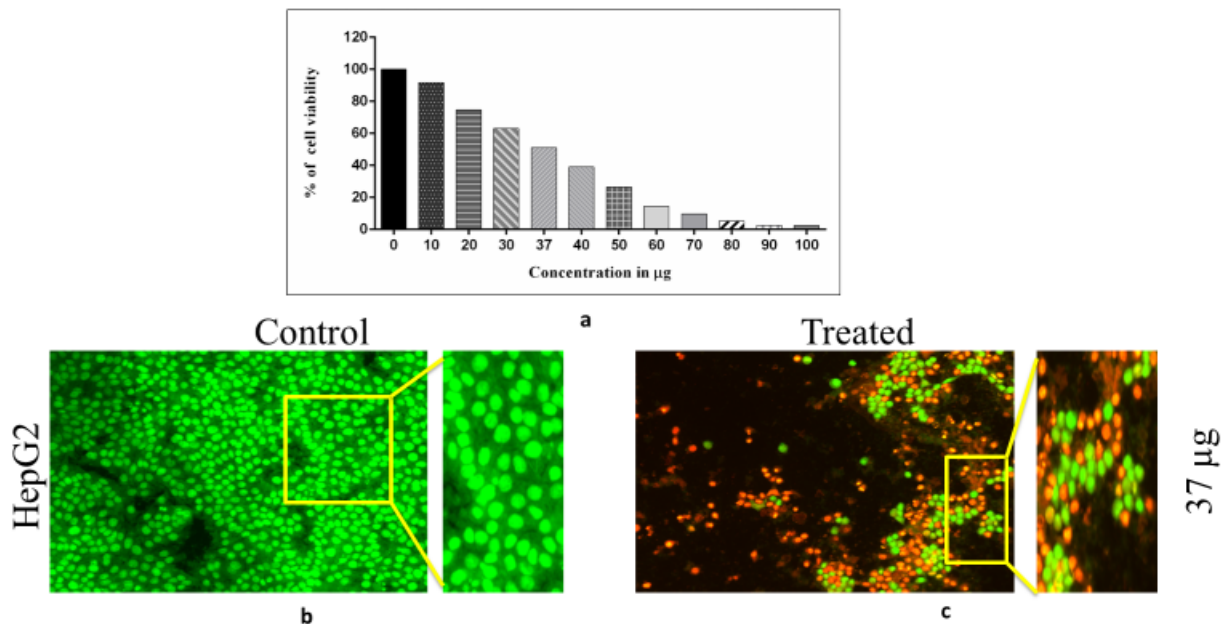


Figure 10. (a) indicates the cytotoxic graphical representation of *Sg*-CuO NPs (10–100 µg/mL) with HepG 2 hepatocellular carcinoma cell lines. (b) presents the control cells, and (c) displays those cells treated with *Sg*-CuO NPs at 37 µg/mL (IC₅₀).

4. Conclusions

S. grandiflora-mediated CuO nanoparticles were green-synthesized and characterized with various advanced techniques, revealing the formation of *Sg*-CuO NPs. It is confirmed that the typical nanoparticle's size was an approximately 33 nm (diameter) and 1051 nm (length) needle shape. Furthermore, free radical scavenging activity, α amylase, and α glucosidase inhibitory activities showed the compound's anti-oxidant and anti-hyperglycemic nature. Moreover, our study confirmed its anti-bacterial, anti-inflammatory, and therapeutic possibilities as a drug with the cytotoxic assay. Nevertheless, its mechanism of action to reduce hyperglycemia and bacterial infection, and its cytotoxicity in different cell lines, need to be further explored. Nonetheless, it displays enormous potential for development as a treatment option for hyperglycemia and its complications.

Author Contributions: Conceptualization, K.R. and V.D.R.; methodology, K.R. and S.P.; software, M.G.; validation, V.D.R., M.G., K.A.A.-G. and M.N.; formal analysis, K.R.; investigation, K.R.; resources, K.A.A.-G.; data curation, K.R.; writing—original draft preparation, K.R.; writing—review and editing, N.S., M.G., K.A.A.-G. and M.N.; supervision, V.D.R.; funding acquisition, K.A.A.-G. All authors have read and agreed to the published version of the manuscript.

Funding: This research received funding from King Saud University with the No. RSP2023R48.

Institutional Review Board Statement: Not applicable.

Informed Consent Statement: Not applicable.

Data Availability Statement: The datasets are available from the corresponding author upon reasonable request.

Acknowledgments: The authors are grateful to the Vellore Institute of Technology–Vellore for providing the laboratory facilities. The authors express their sincere appreciation to the Researchers supporting Project Number (RSP2023R48) at King Saud University, Riyadh, Saudi Arabia. Authors thank the Peoples Friendship University of Russia (RUDN University), Russia.

Conflicts of Interest: The authors declare no conflict of interest.

References

1. Ameen, S.; Rajesh, N.; Anjum, S.M.; Khadri, H.; Riazunnisa, K.; Mohammed, A.; Kari, Z.A. Antioxidant, Antibacterial, and Anti-Diabetic Activity of Green Synthesized Copper Nanoparticles of *Cocculus hirsutus* (Menispermaceae). *Appl. Biochem. Biotechnol.* **2022**, *194*, 4424–4438. [[CrossRef](#)] [[PubMed](#)]
2. Rajeshkumar, S.; Menon, S.; Venkat Kumar, S.; Ponnaniakamideen, M.; Ali, D.; Arunachalam, K. Anti-Inflammatory and Antimicrobial Potential of *Cissus quadrangularis*-Assisted Copper Oxide Nanoparticles. *J. Nanomater.* **2021**, *2021*, 1–11. [[CrossRef](#)]
3. Amjad, R.; Mubeen, B.; Ali, S.S.; Imam, S.S.; Alshehri, S.; Ghoneim, M.M.; Alzarea, S.I.; Rasool, R.; Ullah, I.; Nadeem, M.S.; et al. Green Synthesis and Characterization of Copper Nanoparticles Using *Fortunella margarita* Leaves. *Polymers* **2021**, *13*, 4364. [[CrossRef](#)]
4. Thiruvengadam, M.; Chung, I.M.; Gomathi, T.; Ansari, M.A.; Gopiesh Khanna, V.; Babu, V.; Rajakumar, G. Synthesis, Characterization and Pharmacological Potential of Green Synthesized Copper Nanoparticles. *Bioprocess Biosyst. Eng.* **2019**, *42*, 1769–1777. [[CrossRef](#)] [[PubMed](#)]
5. Anantaworasakul, P.; Klayraung, S.; Okonogi, S. Antibacterial Activities of *Sesbania Grandiflora* Extracts. *Drug Discov. Ther.* **2011**, *5*, 12–17. [[CrossRef](#)] [[PubMed](#)]
6. Rajendran, S.P.; Sengodan, K. Synthesis and Characterization of Zinc Oxide and Iron Oxide Nanoparticles Using *Sesbania grandiflora* Leaf Extract as Reducing Agent. *J. Nanosci.* **2017**, *2017*, 1–7. [[CrossRef](#)]
7. Sureka, C.; Elango, V.; Al-ghamdi, S.; Aldossari, K.K.; Alsaidan, M.; Gedday, A.; Abdelaziz, M.A.; Peer, A.; Ramesh, T. Ameliorative Property of *Sesbania grandiflora* on Carbohydrate Metabolic Enzymes in the Liver and Kidney of Streptozotocin-Induced Diabetic Rats. *Saudi J. Biol. Sci.* **2021**, *28*, 3669–3677. [[CrossRef](#)]
8. Zamroni, A.; Widjanarko, S.B.; Rifa, M. Antihyperglycemic Effect of *Sesbania grandiflora* Seed Decoction on Streptozotocin-Induced Diabetic Mice: Inflammatory Status and the Role of Interleukin-10. *AIP Conf. Proc.* **2017**, *1844*, 020015. [[CrossRef](#)]
9. Loganayaki, N.; Suganya, N.; Manian, S. Evaluation of Edible Flowers of Agathi (*Sesbania grandiflora* L. Fabaceae) for in Vivo Anti-Inflammatory and Analgesic, and in Vitro Anti-oxidant Potential. *Food Sci. Biotechnol.* **2012**, *21*, 509–517. [[CrossRef](#)]
10. Karthika, V.; Kaleeswarran, P.; Gopinath, K.; Arumugam, A.; Govindarajan, M.; Alharbi, N.S.; Khaled, J.M.; Al-anbr, M.N.; Benelli, G. Biocompatible properties of nano-drug carriers using TiO₂-Au embedded on multiwall carbon nanotubes for targeted drug delivery. *Mater. Sci. Eng. C* **2018**, *90*, 589–601. [[CrossRef](#)]
11. Mallikarjuna, K.; Blasubramaniyam, K.; Narasimha, G.; Haekyoung, K. Phyto-Synthesis and Antibacterial Studies of Bio-Based Silver Nanoparticles Using *Sesbania grandiflora* (Avisa) Leaf Tea Extract. *Mater. Res. Express* **2018**, *5*, 015054. [[CrossRef](#)]
12. Berbudi, A.; Rahmadika, N.; Tjahjadi, A.I.; Ruslami, R. Type 2 Diabetes and Its Impact on the Immune System. *Curr. Diabetes Rev.* **2019**, *16*, 442–449. [[CrossRef](#)]
13. Akash, M.S.H.; Rehman, K.; Fiayyaz, F.; Sabir, S.; Khurshid, M. Diabetes-Associated Infections: Development of Anti-microbial Resistance and Possible Treatment Strategies. *Arch. Microbiol.* **2020**, *202*, 953–965. [[CrossRef](#)] [[PubMed](#)]
14. Thurlow, L.R.; Stephens, A.C.; Hurley, K.E.; Richardson, A.R. Lack of Nutritional Immunity in Diabetic Skin Infections Promotes *Staphylococcus aureus* Virulence. *Sci. Adv.* **2020**, *6*, eabc5569. [[CrossRef](#)]
15. Mohanty, S.; Kamolvit, W.; Scheffschick, A.; Björklund, A.; Tovi, J.; Espinosa, A.; Brismar, K.; Nyström, T.; Schröder, J.M.; Östenson, C.G.; et al. Diabetes Downregulates the Anti-microbial Peptide Psoriasin and Increases *E. coli* Burden in the Urinary Bladder. *Nat. Commun.* **2022**, *13*, 4983. [[CrossRef](#)]
16. Segura-Cerda, C.A.; López-Romero, W.; Flores-Valdez, M.A. Changes in Host Response to *Mycobacterium tuberculosis* Infection Associated With Type 2 Diabetes: Beyond Hyperglycemia. *Front. Cell Infect. Microbiol.* **2019**, *9*, 342. [[CrossRef](#)]
17. Chávez-Reyes, J.; Escárcega-González, C.E.; Chavira-Suárez, E.; León-Buitimea, A.; Vázquez-León, P.; Morones-Ramírez, J.R.; Villalón, C.M.; Quintanar-Stephano, A.; Marichal-Cancino, B.A. Susceptibility for Some Infectious Diseases in Patients With Diabetes: The Key Role of Glycemia. *Front. Public Health* **2021**, *9*, 559595. [[CrossRef](#)]
18. Sachdeva, S.; Desai, R.; Gupta, U.; Prakash, A.; Jain, A.; Aggarwal, A. Admission Hyperglycemia in Non-Diabetics Predicts Mortality and Disease Severity in COVID-19: A Pooled Analysis and Meta-Summary of Literature. *SN Compr. Clin. Med.* **2020**, *2*, 2161–2166. [[CrossRef](#)]
19. Farooq, N.; Chuan, B.; Mahmud, H.; El Khoudary, S.R.; Nouraei, S.M.; Evankovich, J.; Yang, L.; Dunlap, D.; Bain, W.; Kitsios, G.; et al. Association of the Systemic Host Immune Response with Acute Hyperglycemia in Mechanically Ventilated Septic Patients. *PLoS ONE* **2021**, *16*, e0248853. [[CrossRef](#)]
20. Dey, A.; Lakshmanan, J. The Role of Anti-oxidants and Other Agents in Alleviating Hyperglycemia Mediated Oxidative Stress and Injury in Liver. *Food Funct.* **2013**, *4*, 1148–1184. [[CrossRef](#)]
21. Asadi, S.; Moradi, M.N.; Khyripour, N.; Goodarzi, M.T.; Mahmoodi, M. Resveratrol Attenuates Copper and Zinc Homeostasis and Ameliorates Oxidative Stress in Type 2 Diabetic Rats. *Biol. Trace Elem. Res.* **2017**, *177*, 132–138. [[CrossRef](#)] [[PubMed](#)]

22. Weksler-Zangen, S.; Jörens, A.; Tarsi-Chen, L.; Vernea, F.; Aharon-Hananel, G.; Saada, A.; Lenzen, S.; Raz, I. Dietary Copper Supplementation Restores β -Cell Function of Cohen Diabetic Rats: A Link between Mitochondrial Function and Glucose-Stimulated Insulin Secretion. *Am. J. Physiol.-Endocrinol. Metab.* **2013**, *304*, 1023–1034. [[CrossRef](#)] [[PubMed](#)]
23. Ghadi, F.E.; Ghara, A.R.; Naeimi, A. Phytochemical Fabrication, Characterization, and Anti-oxidant Application of Copper and Cobalt Oxides Nanoparticles Using Sesbania Sesban Plant. *Chem. Pap.* **2018**, *72*, 2859–2869. [[CrossRef](#)]
24. Rajamma, R.; Nair, S.G.; Khadar, F.A.; Baskaran, B. Antibacterial and Anticancer Activity of Biosynthesised CuO Nanoparticles. *IET Nanobiotechnol.* **2020**, *14*, 833–838. [[CrossRef](#)]
25. Das, P.E.; Abu-yousef, I.A.; Majdalawieh, A.F.; Narasimhan, S. Green Synthesis of Encapsulated Copper Nanoparticles Using a Hydroalcoholic Extract of *Moringa oleifera* Leaves and Assessment of Their Anti-oxidant and Anti-Microbial Activities Supplementary Figure 1. Resazurin Microtiter Assay Pla. *Molecule* **2020**, *25*, 555. [[CrossRef](#)]
26. Iqbal, E.; Salim, A.K.; Lim, B.L. Phytochemical Screening, Total Phenolics and Antioxidant Activities of Bark and Leaf Extracts of *Goniothalamus velutinus* (Airy Shaw) from Brunei Darussalam. *J. King Saud Univ.* **2015**, *27*, 224–232. [[CrossRef](#)]
27. Kancherla, N.; Dhakshinamoothi, A.; Chitra, K.; Komaram, R.B. Preliminary Analysis of Phytoconstituents and Evaluation of Anthelmintic Property of *Cayratia auriculata* (In Vitro). *Maedica* **2019**, *14*, 350–356. [[CrossRef](#)]
28. Le Thi, V.A.; Nguyen, N.L.; Nguyen, Q.H.; Van Dong, Q.; Do, T.Y.; Nguyen, K.O.T. Phytochemical Screening and Potential Anti-bacterial Activity of Defatted and Nondefatted Methanolic Extracts of Xao Tam Phan (Paramignya Trimera (Oliv.) Guillaum) Peels against Multidrug-Resistant Bacteria. *Scientifica* **2021**, *2021*, 4233615. [[CrossRef](#)]
29. Rajakumar, G.; Thiruvengadam, M.; Mydhili, G. Green Approach for Synthesis of Zinc Oxide Nanoparticles from *Andrographis paniculata* Leaf Extract and Evaluation of Their Anti-oxidant, Anti-Diabetic, and Anti-Inflammatory Activities. *Bioprocess Biosyst. Eng.* **2018**, *41*, 21–30. [[CrossRef](#)]
30. Das, G.; Patra, J.K.; Debnath, T.; Ansari, A. Investigation of Anti-oxidant, Anti-bacterial, Anti-diabetic, and Cytotoxicity Potential of Silver Nanoparticles Synthesized Using the Outer Peel Extract of *Ananas comosus* (L.). *PLoS ONE* **2019**, *14*, e0220950. [[CrossRef](#)]
31. Rehana, D.; Senthil, D.M.R.; Kalilur, K.A. In Vitro Anti-oxidant and Anti-diabetic Activities of Zinc Oxide Nanoparticles Synthesized Using Different Plant Extracts. *Bioprocess Biosyst. Eng.* **2017**, *40*, 943–957. [[CrossRef](#)] [[PubMed](#)]
32. Anokwah, D.; Kwatia, E.A.; Amponsah, I.K.; Jibira, Y.; Harley, B.K.; Ameyaw, E.O.; Obese, E.; Biney, R.P.; Mensah, A.Y. Evaluation of the Anti-Inflammatory and Antioxidant Potential of the Stem Bark Extract and Some Constituents of *Aidia genipiflora* (DC.) Dandy (Rubiaceae). *Heliyon* **2022**, *8*, e10082. [[CrossRef](#)] [[PubMed](#)]
33. Sheik Mydeen, S.; Raj Kumar, R.; Kottaisamy, M.; Vasantha, V.S. Biosynthesis of ZnO Nanoparticles through Extract from *Prosopis juliflora* Plant Leaf: Anti-bacterial Activities and a New Approach by Rust-Induced Photocatalysis. *J. Saudi Chem. Soc.* **2020**, *24*, 393–406. [[CrossRef](#)]
34. Pajaniradje, S.; Mohankumar, K.; Pamidimukkala, R.; Subramanian, S.; Rajagopalan, R. Antiproliferative and Apoptotic Effects of *Sesbania grandiflora* Leaves in Human Cancer Cells. *Biomed Res. Int.* **2014**, *2014*, 474953. [[CrossRef](#)] [[PubMed](#)]
35. Faisal, S.; Jan, H.; Abdullah; Alam, I.; Rizwan, M.; Hussain, Z.; Sultana, K.; Ali, Z.; Uddin, M.N. In Vivo Analgesic, Anti-Inflammatory, and Anti-Diabetic Screening of *Bacopa monnieri*-Synthesized Copper Oxide Nanoparticles. *ACS Omega* **2022**, *7*, 4071–4082. [[CrossRef](#)] [[PubMed](#)]
36. Saligedo, T.S.; Muleta, G.G.; Tsega, T.W.; Tadele, K.T. Green Synthesis of Copper Oxide Nanoparticles Using Eichhornia Crassipes Leaf Extract, Its Anti-bacterial and Photocatalytic Activities. *Curr. Nanomater.* **2022**, *8*, 58–68.
37. Verma, N.; Kumar, N. Synthesis and Biomedical Applications of Copper Oxide Nanoparticles: An Expanding Horizon. *ACS Biomater. Sci. Eng.* **2019**, *5*, 1170–1188. [[CrossRef](#)] [[PubMed](#)]
38. Liu, T.; Xiao, B.; Xiang, F.; Tan, J.; Chen, Z.; Zhang, X.; Wu, C.; Mao, Z.; Luo, G.; Chen, X.; et al. Ultrasmall Copper-Based Nanoparticles for Reactive Oxygen Species Scavenging and Alleviation of Inflammation Related Diseases. *Nat. Commun.* **2020**, *11*, 2788. [[CrossRef](#)]
39. Kheshtzar, R.; Berenjian, A.; Taghizadeh, S.M.; Ghasemi, Y.; Asad, A.G.; Ebrahimezhad, A. Optimization of Reaction Parameters for the Green Synthesis of Zero Valent Iron Nanoparticles Using Pine Tree Needles. *Green Process Synth.* **2019**, *8*, 846–855. [[CrossRef](#)]
40. Noor, S.; Shah, Z.; Javed, A.; Ali, A.; Hussain, S.B.; Zafar, S.; Ali, H.; Muhammad, S.A. A Fungal Based Synthesis Method for Copper Nanoparticles with the Determination of Anticancer, Anti-diabetic and Anti-bacterial Activities. *J. Microbiol. Methods* **2020**, *174*, 105966. [[CrossRef](#)]
41. Ashar, A.; Iqbal, M.; Bhartti, A.I.; Ahmad, Z.M.; Qureshi, K.; Nisar, J.; Bukhari, H.I. Synthesis, Characterization and Photocatalytic Activity of ZnO Flower and Pseudo-Sphere: Nonylphenol Ethoxylate Degradation under UV and Solar Irradiation. *J. Alloys Compd.* **2016**, *678*, 126–136. [[CrossRef](#)]
42. Vijayakumar, G.; Kesavan, H.; Kannan, A.; Arulanandam, D.; Kim, J.H.; Kim, K.J.; Song, H.J.; Kim, H.J.; Rangarajulu, S.K. Phytosynthesis of Copper Nanoparticles Using Extracts of Spices and Their Anti-bacterial Properties. *Processes* **2021**, *9*, 1341. [[CrossRef](#)]
43. Agidew, M.G. Phytochemical Analysis of Some Selected Traditional Medicinal Plants in Ethiopia—Bulletin of the National Research Centre—Full Text. *Bull. Natl. Res. Cent.* **2022**, *46*, 87. [[CrossRef](#)]
44. Marslin, G.; Siram, K.; Maqbool, Q.; Selvakesavan, R.K.; Kruszka, D.; Kachlicki, P.; Franklin, G. Secondary Metabolites in the Green Synthesis of Metallic Nanoparticles. *Materials* **2018**, *11*, 940. [[CrossRef](#)] [[PubMed](#)]

45. Thissera, B.; Visvanathan, R.; Khanfar, M.A.; Qader, M.M.; Hassan, M.H.A.; Hassan, H.M.; Bawazeer, M.; Behery, F.A.; Yaseen, M.; Liyanage, R.; et al. *Sesbania grandiflora* L. Poir Leaves: A Dietary Supplement to Alleviate Type 2 Diabetes through Metabolic Enzymes Inhibition. *South African J. Bot.* **2020**, *130*, 282–299. [[CrossRef](#)]
46. Delavari, N.M.; Gharaei, A.; Mirdar, H.J.; Davari, A.; Rastiannasab, A. Modulatory Effect of Dietary Copper Nanoparticles and Vitamin C Supplementations on Growth Performance, Hematological and Immune Parameters, Oxidative Status, Histology, and Disease Resistance against *Yersinia ruckeri* in Rainbow Trout (*Oncorhynchus Mykiss*). *Fish Physiol. Biochem.* **2022**, *48*, 33–51. [[CrossRef](#)]
47. Newsholme, P.; Cruzat, V.F.; Keane, K.N.; Carlessi, R.; De Bittencourt, P.I.H. Molecular Mechanisms of ROS Production and Oxidative Stress in Diabetes. *Biochem. J.* **2016**, *473*, 4527–4550. [[CrossRef](#)]
48. Ishwarya, R.; Vaseeharan, B.; Anuradha, R.; Rekha, R.; Govindarajan, M.; Alharbi, N.S.; Kadaikunnan, S.; Khaled, J.M.; Benelli, G. Eco-friendly fabrication of Ag nanostructures using the seed extract of *Pedaliium murex*, an ancient Indian medicinal plant: Histopathological effects on the Zika virus vector *Aedes aegypti* and inhibition of biofilm-forming pathogenic bacteria. *J. Photochem. Photobiol. B Biol.* **2017**, *174*, 133–143. [[CrossRef](#)]
49. Gupta, S.; Apte, K.G. Evaluation of Phytochemical, Anti-oxidant and Cytotoxic Potential of *Sesbania grandiflora* Linn. *J. Phytopharm.* **2018**, *7*, 191–198. [[CrossRef](#)]
50. Yuan, T.; Yang, T.; Chen, H.; Fu, D.; Hu, Y.; Wang, J.; Yuan, Q.; Yu, H.; Xu, W.; Xie, X. New Insights into Oxidative Stress and Inflammation during Diabetes Mellitus-Accelerated Atherosclerosis. *Redox Biol.* **2019**, *20*, 247–260. [[CrossRef](#)]
51. Ahmed, N.; Babaei-Jadidi, R.; Howell, S.K.; Thornalley, P.J.; Beisswenger, P.J. Glycated and Oxidized Protein Degradation Products Are Indicators of Fasting and Postprandial Hyperglycemia in Diabetes. *Diabetes Care* **2005**, *28*, 2465–2471. [[CrossRef](#)] [[PubMed](#)]
52. Pouresmaeil, V.; Al Abudi, A.H.; Mahimid, A.H.; Sarafraz Yazdi, M.; Es-haghi, A. Evaluation of Serum Selenium and Copper Levels with Inflammatory Cytokines and Indices of Oxidative Stress in Type 2 Diabetes. *Biol. Trace Elem. Res.* **2023**, *201*, 617–626. [[CrossRef](#)] [[PubMed](#)]
53. Psomas, G. Copper(II) and Zinc(II) Coordination Compounds of Non-Steroidal Anti-Inflammatory Drugs: Structural Features and Anti-oxidant Activity. *Coord. Chem. Rev.* **2020**, *412*, 213259. [[CrossRef](#)]
54. Hussain, A.; AlAjmi, M.F.; Rehman, M.T.; Amir, S.; Husain, F.M.; Alsalme, A.; Siddiqui, M.A.; AlKhedhairi, A.A.; Khan, R.A. Copper(II) Complexes as Potential Anticancer and Nonsteroidal Anti-Inflammatory Agents: In Vitro and in Vivo Studies. *Sci. Rep.* **2019**, *9*, 5237. [[CrossRef](#)]
55. Zhang, R.; Jiang, G.; Gao, Q.; Wang, X.; Wang, Y.; Xu, X.; Yan, W.; Shen, H. Sprayed Copper Peroxide Nanodots for Accelerating Wound Healing in a Multidrug-Resistant Bacteria Infected Diabetic Ulcer. *Nanoscale* **2021**, *13*, 15937–15951. [[CrossRef](#)]
56. Sandoval, C.; Ríos, G.; Sepúlveda, N.; Salvo, J.; Souza-Mello, V.; Fariás, J. Effectiveness of Copper Nanoparticles in Wound Healing Process Using In Vivo and In Vitro Studies: A Systematic Review. *Pharmaceutics* **2022**, *14*, 1838. [[CrossRef](#)]
57. Alam, M.W.; Al Qahtani, H.S.; Souayeh, B.; Ahmed, W.; Albalawi, H.; Farhan, M.; Abuzir, A.; Naeem, S. Novel Copper-Zinc-Manganese Ternary Metal Oxide Nanocomposite as Heterogeneous Catalyst for Glucose Sensor and Antibacterial Activity. *Antioxidants* **2022**, *11*, 1064. [[CrossRef](#)]
58. Wu, S.; Rajeshkumar, S.; Madasamy, M.; Mahendran, V. Green Synthesis of Copper Nanoparticles Using *Cissus vitiginea* and Its Anti-oxidant and Anti-bacterial Activity against Urinary Tract Infection Pathogens. *Artif. Cells Nanomed. Biotechnol.* **2020**, *48*, 1153–1158. [[CrossRef](#)]
59. Gandhi, A.D.; Vizhi, D.K.; Lavanya, K.; Kalpana, V.N.; Devi Rajeswari, V.; Babujanarthanam, R. In Vitro Anti-Biofilm and Anti-Bacterial Activity of *Sesbania Grandiflora* Extract against *Staphylococcus aureus*. *Biochem. Biophys. Reports* **2017**, *12*, 193–197. [[CrossRef](#)]
60. Gupta, R.; Polaka, S.; Rajpoot, K.; Tekade, M.; Tekade, R.K.; Shirma, M.C. Importance of Toxicity Testing in Drug Discovery and Research. In *Pharmacokinetic and Toxicological Considerations*; Academic Press: Cambridge, MA, USA, 2022.
61. Chakrabarti, R.; Kundu, S.; Kumar, S.; Chakrabarti, R. Vitamin A as an Enzyme That Catalyzes the Reduction of MTT to Formazan by Vitamin C. *J. Cell Biochem.* **2001**, *80*, 133–138. [[CrossRef](#)]

Disclaimer/Publisher's Note: The statements, opinions and data contained in all publications are solely those of the individual author(s) and contributor(s) and not of MDPI and/or the editor(s). MDPI and/or the editor(s) disclaim responsibility for any injury to people or property resulting from any ideas, methods, instructions or products referred to in the content.